RESEARCH PAPER

Biphasic modulation by mGlu₅ receptors of TRPV1-mediated intracellular calcium elevation in sensory neurons contributes to heat sensitivity

T Masuoka[1], T Nakamura[1], M Kudo[1], J Yoshida[1], Y Takaoka[1], N Kato[2], T Ishibashi[1,3], N Imaizumi[1] and M Nishio[1]

Departments of [1]Pharmacology and [2]Physiology I, School of Medicine, and [3]Pharmacology, School of Nursing, Kanazawa Medical University, Uchinada, Japan

BACKGROUND AND PURPOSE

Elevation of glutamate, an excitatory amino acid, during inflammation and injury plays a crucial role in the reception and transmission of sensory information via ionotropic and metabotropic receptors. This study aimed to investigate the mechanisms underlying the biphasic effects of metabotropic glutamate mGlu₅ receptor activation on responses to noxious heat.

EXPERIMENTAL APPROACH

We assessed the effects of intraplantar quisqualate, a non-selective glutamate receptor agonist, on heat and mechanical pain behaviours in mice. In addition, the effects of quisqualate on the intracellular calcium response and on membrane currents mediated by TRPV1 channels, were examined in cultured dorsal root ganglion neurons from mice.

KEY RESULTS

Activation of mGlu₅ receptors in hind paw transiently increased, then decreased, the response to noxious heat. In sensory neurons, activation of mGlu₅ receptors potentiated TRPV1-mediated intracellular calcium elevation, while terminating activation of mGlu₅ receptors depressed it. TRPV1-induced currents were potentiated by activation of mGlu₅ receptors under voltage clamp conditions and these disappeared after washout. However, voltage-gated calcium currents were inhibited by the mGlu₅ receptor agonist, even after washout.

CONCLUSIONS AND IMPLICATIONS

These results suggest that, in sensory neurons, mGlu₅ receptors biphasically modulate TRPV1-mediated intracellular calcium response via transient potentiation of TRPV1 channel-induced currents and persistent inhibition of voltage-gated calcium currents, contributing to heat hyper- and hypoalgesia.

Abbreviations

5′-IRTX, 5′-iodoresiniferatoxin; ACSF, artificial CSF; [Ca²⁺]ᵢ, intracellular free Ca²⁺ concentration; CPCCOEt, 7-(hydroxyimino) cyclopropa[b]chromen-1a-carboxylate ethyl ester; DHPG, 3,5-dihydroxyphenylglycine; DRG, dorsal root ganglion; MPEP, 2-methyl-6-(phenylethynyl)pyridine; VGCC, voltage-gated calcium channel

Tables of Links

TARGETS	LIGANDS
GPCR[a]	5′-IRTX, 5′-iodoresiniferatoxin
mGlu$_5$ receptors	AMPA
Ion channels[b]	Capsaicin
VGCC, voltage-gated calcium channels	CPCCOEt, 7-(hydroxyimino) cyclopropa[b]chromen-1a-carboxylate ethyl ester
N-type Ca channels	DHPG, 3,5-dihydroxyphenylglycine
L-type Ca channels	Glutamate
TRPV1 channels	MPEP, 2-methyl-6-(phenylethynyl)pyridine
Ligand-gated ion channels[c]	Quisqualate
AMPA receptors	

These Tables list key protein targets and ligands in this article which are hyperlinked to corresponding entries in http://www.guidetopharmacology.org, the common portal for data from the IUPHAR/BPS Guide to PHARMACOLOGY (Pawson *et al.*, 2014) and are permanently archived in the Concise Guide to PHARMACOLOGY 2013/14 ([a,b,c]Alexander *et al.*, 2013a,b,c).

Introduction

L-glutamate, the most prominent excitatory neurotransmitter in the CNS, acts through ligand-gated ionotropic and metabotropic receptors to regulate a variety of normal brain and spinal functions. Dysfunction of the glutamatergic system is likely to be involved in the development of psychiatric disorders (Dölen *et al.*, 2007; Ménard and Quirion, 2012) and persistent pain (Liu and Salter, 2010; Chiechio and Nicoletti, 2012). Inflammation and nerve injury in the periphery causes glutamate release from sensory neurons, glia, and damaged cells in the spinal cord and peripheral tissue (Omote *et al.*, 1998; Lawand *et al.*, 2000; Liu and Salter, 2010), which in turn causes inflammatory and neuropathic pain. Many studies have indicated that spinal metabotropic glutamate mGlu$_5$ receptors contribute to nociceptive processing during this pain (Walker *et al.*, 2001; Hudson *et al.*, 2002; Guo *et al.*, 2004; Yan *et al.*, 2009; Li *et al.*, 2010; Liu *et al.*, 2012). Morphological evidence has shown that mGlu$_5$ receptors are also expressed in dorsal root ganglion (DRG) cell bodies and unmyelinated afferents in peripheral tissue (Bhave *et al.*, 2001). Systemic injection of an mGlu$_{1/5}$ receptor agonist leads to increased sensitivity to noxious heat, or thermal hyperalgesia, and selective mGlu$_1$ and mGlu$_5$ receptor antagonists attenuate formalin-induced pain (Bhave *et al.*, 2001). Therefore, the mGlu$_5$ receptors in primary afferent fibres may be a potential therapeutic target for the prevention and treatment of neuropathic and inflammatory pain.

The non-selective cation TRPV1 channel is activated by capsaicin, acidic pH (pH < 6.0), noxious heat (>42°C), and endovanilloid compounds (Caterina *et al.*, 1997). TRPV1 channels are highly expressed in the peripheral nervous system and highly enriched in unmyelinated C-fibres, myelinated Aδ fibres, and nociceptor somata in trigeminal, vagal, and DRG (Han *et al.*, 2013; Mitchell *et al.*, 2014). Thus, TRPV1 channels have the potential to integrate responses to multiple noxious stimuli, and play an important role in pain sensation. Recent research suggests there may be an interaction between mGlu$_5$ receptors and TRPV1 channels in cell physiology and pain behaviour, as mGlu$_5$ receptors directly acti-

vate TRPV1 channels in presynaptic terminals of the dorsal horn in rats (Kim *et al.*, 2009). Hyperalgesia induced by activation of mGlu$_5$ receptors may be mediated by TRPV1 channel function, as perineural pretreatment with 1% capsaicin significantly reduced pain-related behaviour induced by mGlu$_5$ receptor agonists (Jung *et al.*, 2011). However, the details of peripheral mGlu$_5$ receptor function and mGlu$_5$ receptor – TRPV1 channel interactions in DRG neurons remain unclear.

Here, we show that mGlu$_5$ receptors biphasically modulate the TRPV1 channel-mediated intracellular calcium response in peripheral sensory neurons, contributing to hyper- and hypoalgesia in mice.

Methods

All animal care and experimental procedures were in accordance with 'Guiding Principles for the Care and Use of Laboratory Animals' set by the Japanese Pharmacological Society and approved by the Ethics Committee of Kanazawa Medical University. All studies involving animals are reported in accordance with the ARRIVE guidelines for reporting experiments involving animals (Kilkenny *et al.*, 2010; McGrath *et al.*, 2010). A total of 126 animals were used in the experiments described here.

Behavioural testing

Pain behaviours, in response to thermal and mechanical stimuli, were measured in 8-week-old C57BL/6J male mice (SLC, Shizuoka, Japan). Thermal sensitivity was assessed using the hot plate test. The heated surface of the plate was kept at a temperature of 55 ± 0.1°C (Model-DS 37, Ugo Basile, Comerio, Italy), as measured by a built-in digital thermometer (accurate to 0.1°C), and verified by a surface thermometer. Mice were placed on the hot plate and surrounded by a clear acrylic cage. The latency to respond was measured as the time it took for the mouse to either lick, flick or bite its hind paw, or jump (whichever happened first). After a response, the mouse was immediately removed from the hot plate and

returned to its home cage. In the absence of paw licking or jumping, a 20 s cut-off was used to prevent tissue damage. The tests were performed just prior to intraplantar drug injection, as well as 15 min and 4 h after injection. Mechanical sensitivity was assessed by measuring paw withdrawal thresholds using calibrated von Frey filaments (Aesthesio®, DanMic Global, LLC, San Jose, CA, USA). Mice were acclimatized to a clear acrylic cylinder (outer diameter 19 cm, height 13 cm) placed on an elevated wire-mesh platform, which allowed access to the ventral surface of the hind paws. Filaments (0.07–2.0 g) were presented perpendicular to the plantar surface of the injected paw and held in this position for 5 s, using enough force to cause a slight bend in the filament. Positive responses were recorded when there was an abrupt withdrawal of the hind paw, or flinching behaviour, immediately following removal of the stimulus. A median paw withdrawal threshold was determined using an adaptation of Dixon's up-and-down method (Chaplan *et al.*, 1994).

DRG cultures

For dissection and plating of DRG, we followed a protocol previously reported by Callaghan *et al.* (2008). To prepare stable cultured neurons, younger mice were used in the culture experiment compared with behavioural testing. Six- to 14-day-old C57BL/6J mice (SLC, Shizuoka, Japan) were anaesthetized with isoflurane, and DRG were rapidly dissected from all spinal levels in ice-cold Ca^{2+}/Mg^{2+}-free artificial CSF (ACSF; composition given below). DRG neurons were dissociated following treatment with Ca^{2+}/Mg^{2+}-free ACSF containing 0.1% type II collagenase (240 unit mg^{-1}; Worthington Biochemical, Co., Lakewood, NJ, USA), 0.1% trypsin (Gibco, San Diego, CA, USA), and 0.01% DNase I (Sigma, St. Louis, MO, USA) for 1 h at 37 °C. Cells were gently triturated in DMEM (D6429; Sigma) containing 10% horse serum (Gibco), 5% FCS (Gibco) and 1% penicillin-streptomycin (Wako, Osaka, Japan). Agglutinative cells were removed using a 100 μm Cell Strainer (BD Biosciences, San Jose, CA, USA) and the remaining cells plated on 13 mm diameter coverslips coated with poly-L-lysine (Matsunami Glass Ind., Osaka, Japan). Calcium imaging and patch-clamp recording were performed 2–3 days after dissociation.

Calcium imaging

Imaging was conducted as described previously (Yoshida *et al.*, 2005). For microscopic fluorometric measurement of intracellular free Ca^{2+} concentrations ($[Ca^{2+}]_i$), DRG neuronal cultures were washed twice with ACSF (containing 138.6 mM NaCl, 3.35 mM KCl, 21 mM $NaHCO_3$, 9.9 mM glucose, 0.6 mM NaH_2PO_4, 2.5 mM $CaCl_2$, and 1 mM $MgCl_2$), gassed with a mixture of 95% O_2 and 5% CO_2 (pH 7.4), and incubated for 30 min in the dark at room temperature (25 ± 2°C) in a solution with 3 μM of fura-2-acetoxymethyl ester (Fura-2/AM; Dojindo Laboratories, Kumamoto, Japan) and 0.005% Cremophore EL. After incubation, cells were washed in ACSF for 30 min and culture dishes placed on the stage of an inverted microscope (ECLIPSE TE 300, Nikon, Tokyo, Japan) equipped with a 20 × S-fluor objective. Fluorescence images were recorded and analysed using a video image analysis system (ARGUS/HiSCA, Hamamatsu Photonics, Hamamatsu, Japan). Experimental agents were dissolved in ACSF and applied by continuous perfusion (2 mL·min⁻¹) using a peristaltic pump. When cadmium chloride was used to block Ca^{2+} channels, NaH_2PO_4 was replaced to NaCl in the ACSF in order to prevent cadmium precipitation. Image pairs were captured at 5 s intervals. Fura-2 fluorescence was monitored at an emission wavelength of 510 nm by exciting Fura-2 at, alternatively, 340 and 380 nm. The 340–380 nm fluorescence ratio (F340/F380) was used to indicate changes in $[Ca^{2+}]_i$.

Whole-cell recording

Cultured neurons were plated onto coverslips, transferred to the recording chamber, and superfused with 30°C ACSF. Neurons were visually identified using a 60 × water immersion objective attached to an upright microscope (Axioskop 2 FS, Carl Zeiss, Oberkochen, Germany). Pipettes for whole-cell recordings were made from borosilicate glass capillaries (1.5 mm outer diameter; World Precision Instruments, Inc., Sarasota, FL, USS). Patch pipettes (4.6–6.5 MΩ) were filled with an internal solution containing 120 mM KCH_3SO_3, 5 mM KCl, 10 mM K-EGTA, 5 mM Na-HEPES, 3 mM Mg-ATP and 0.4 mM Na-GTP (pH 7.4). Series resistance was 8–20 MΩ, which was monitored throughout recording. Membrane currents were recorded in a whole-cell configuration using an Axoclamp 700A amplifier and pCLAMP 10 software (Axon Instruments, Foster City, CA, USA), digitized, and stored on a computer disk for off-line analysis. To record TRPV1 currents, capsaicin (10 μM) was applied to cells using an air pressure injection through the pipette (Pneumatic PicoPump, PV830; World Precision Instruments, Inc., Sarasota, FL, USA).

To record voltage-gated calcium channel (VGCC) currents, an extracellular solution containing 145 mM tetraethyllammonium (TEA) chloride, 10 mM TEA-HEPES, 15 mM glucose, and 10 mM $CaCl_2$ (pH 7.4) was perfused at a rate of 1–2 mL·min⁻¹. Patch pipettes (3.5–5.0 MΩ) were filled with an internal solution containing 120 mM $CsCH_3SO_3$, 10 mM Cs-EGTA, 10 mM Cs-HEPES, 1 mM $CaCl_2$, 4 mM Mg-ATP, and 0.3 mM Na-GTP (pH 7.4). To evoke VGCC currents, a series of 10 mV, 80 ms depolarizing steps were applied every 20 s, from a holding potential of –80 mV to +70 mV (Fig. 4A). Drugs effects on VGCC currents were tested during perfusion or 10–30 min after washout. A series of recordings from a single DRG neuron were performed only once because VGCCs are easily desensitized by repetitive stimulation.

Data analysis

Results are expressed as mean ± SEM, and *n* represents the number of the cells or animals examined. Data were analysed using StatView (SAS Institute Inc., Cary, NC, USA) and SigmaPlot 8.0.2 (SPSS, Inc., Drunen, The Netherlands). Statistical significance was assessed by using a one-way ANOVA with *post hoc* Dunnett's test. $P < 0.05$ was considered statistically significant.

Materials

Quisqualic acid and capsaicin (a TRPV1 channel activator) were obtained from Sigma, while (S)-3,5-dihydroxyphenylglycine (DHPG, an mGlu$_{1/5}$ receptor agonist), α-amino-3-hydroxy-5-methylisoxazole-4-propionic acid (AMPA, an AMPA receptor agonist), 7-(hydroxyimino)cyclopropa[b]chromen-1a-carboxylate ethyl ester (CPCCOEt,

a selective negative allosteric mGlu$_1$ receptor modulator), 2-methyl-6-(phenylethynyl)pyridine (MPEP, a selective negative allosteric mGlu$_5$ receptor modulator), and 5'-iodoresiniferatoxin (5'-IRTX, a TRPV1 channel blocker) were obtained from Tocris Cookson (Bristol, UK).

Results

Intraplantar injection of quisqualate causes heat hyper- and hypoalgesia via activation of mGlu$_5$ receptors

We examined the effects of intraplantar injection of quisqualate on hot plate and von Frey responses in mice

(Figure 1). Quisqualate is a non-selective glutamate receptor agonist which can activate AMPA receptors (Stawski *et al.*, 2010) and group I metabotropic glutamate receptors (Abe *et al.*, 1992). In the hot plate test, intraplantar quisqualate (4 nmol per paw) significantly decreased the latency to shake, lick or jump on the hot plate when mice were tested 15 min after injection ($F_{(3,28)} = 3.496$, $P = 0.0414$), indicating heat hyperalgesia (Figure 1B). In contrast, when mice were tested 4 h after injection, this dose significantly increased latency to respond ($F_{(3,28)} = 3.506$, $P = 0.0453$), indicative of heat hypoalgesia (Figure 1C). These hyper- and hypoalgesic effects vanished with concurrent injection of MPEP (5 nmol per paw), a selective negative allosteric modulator of mGlu$_5$ receptors. Intraplantar 5'-IRTX (0.01 nmol per paw) significantly
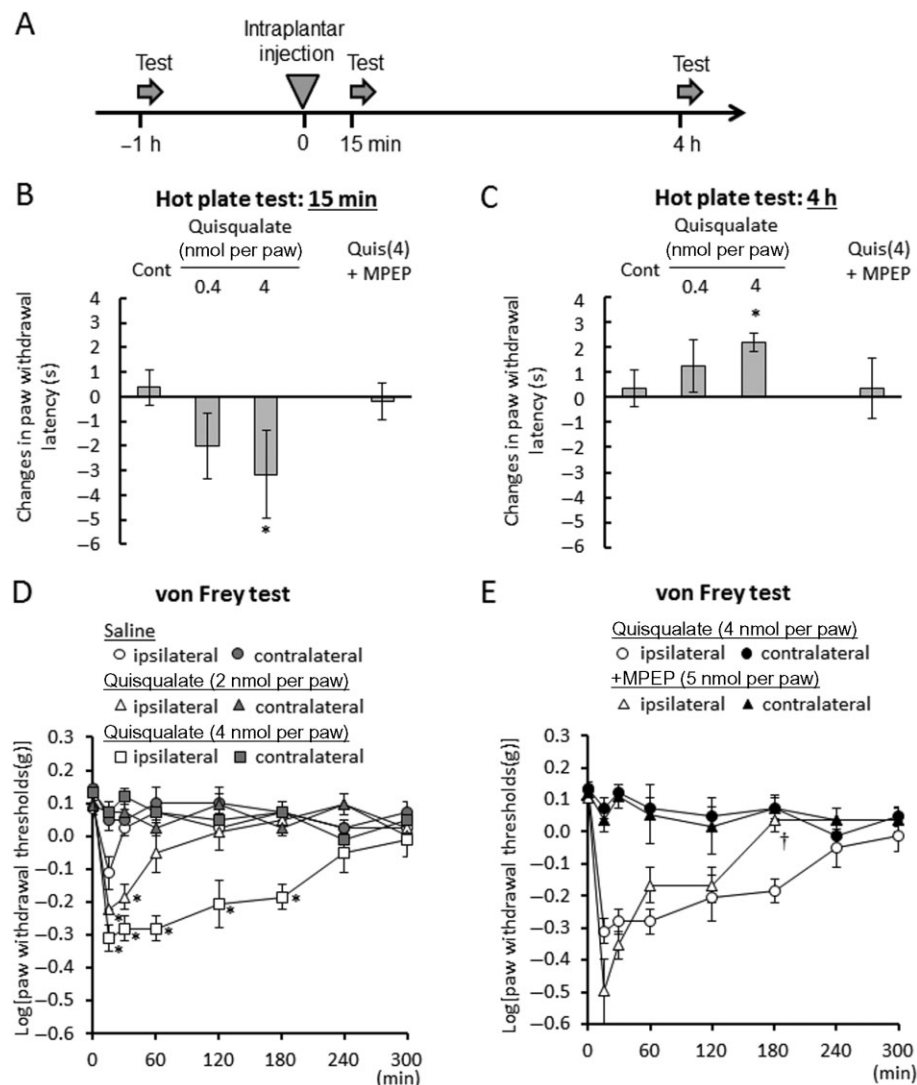

Figure 1

Effects of intraplantar quisqualate injection on hot plate and von Frey's test in mice. (A) Experimental design of hot plate test. Changes in latency to shake, lick or jump after placement on hot plate (55.0 ± 0.2°C) 15 min (B) or 4 h (C) after injection of glutamatergic drugs. Eight mice were used in each group. (D) Time course of mechanical hyperalgesia induced by intraplantar injection of quisqualate. *$P < 0.05$ significantly different from control. (E) Effect of MPEP on quisqualate-induced mechanical allodynia. Six mice were used in each group. Data presented as mean ± SEM. *$P < 0.05$ significantly different from ipsilateral paw in saline group, †$P < 0.05$ significantly different from ipsilateral paw in quisqualate group (4 nmol per paw).

increased the latency to respond 15 min ($F_{(1,14)}$ = 5.243, P = 0.0381) and 4 h ($F_{(1,14)}$ = 29.566, P < 0.0001) after injection, indicating heat hypoalgesia (Supporting Information Fig. S1). Intraplantar quisqualate resulted in significant decreases in paw withdrawal thresholds on the von Frey test, compared with ipsilateral, saline-treated paws, representing induction of mechanical hypersensitivity. These decreases were observed following 2 and 4 nmol per paw quisqualate 15 min ($F_{(2,15)}$ = 15.680; 2 nmol per paw, P = 0.012; 4 nmol per paw, P = 0.0001) and 30 min ($F_{(2,15)}$ = 21.378; 2 nmol per paw, P = 0.0005; 4 nmol per paw, P < 0.0001) after injection (Figure 1D). A dose of 4 nmol per paw quisqualate resulted in decreases in paw withdrawal threshold 60 min ($F_{(2,15)}$ = 16.043, P < 0.0001), 120 min ($F_{(2,15)}$ = 5.644, P = 0.0093) and 180 min ($F_{(2,15)}$ = 17.554, P < 0.0001) after injection (Figure 1D). The mechanical hypersensitivity induced by intraplantar quisqualate was partially decreased 60–180 min after concurrent injection of MPEP, and significantly antagonized after 180 min ($F_{(1, 10)}$ = 22.038, P = 0.0008, against ipsilateral paw in quisqualate group, Figure 1E).

Activation of mGlu5 receptors potentiates capsaicin-induced elevation in intracellular calcium in cultured DRG neurons

We measured $[Ca^{2+}]_i$ in cultured DRG neurons using Fura-2/AM dye. Perfusion of capsaicin (0.5 μM, a TRPV1 channel activator) induced an increase in $[Ca^{2+}]_i$ in half of the cultured mouse DRG neurons (Figure 2 A, E and F); this increase was completely blocked by 1 μM 5'-IRTX, a TRPV1 channel blocker (Figure 2C). Thus, capsaicin-induced calcium elevation appears to be mediated by TRPV1 channel activation. Glutamate acts through a variety of ionotropic (NMDA, AMPA and kainate) and metabotropic receptors ($mGlu_{1-8}$) (Kew and Kemp, 2005). In the present study, perfusion of glutamate (30 μM) and quisqualate (10 μM) significantly potentiated the capsaicin-induced $[Ca^{2+}]_i$ increase in DRG neurons (glutamate: $F_{(1,99)}$ = 26.73, P < 0.0001; quisqualate: $F_{(3,190)}$ = 8.815, P < 0.0001, Figure 2D–G), but did not change the ratio of capsaicin-sensitive neurons. Glutamate, or quisqualate, alone produced no change in $[Ca^{2+}]_i$ in any of the neurons (Figure 2H). To evaluate changes in maximal effect at high concentrations (E_{max}) and concentration needed to give half-maximal effect (EC_{50}) for capsaicin during quisqualate application, dose–response curves for capsaicin (0.03–3.0 μM) were produced (Figure 3A). The presence of quisqualate caused an obvious and significant increase in E_{max} ($F_{(1,49)}$ = 29.46, P < 0.0001, Figure 3B), and significantly decreased EC_{50} ($F_{(1,49)}$ = 4.282, P = 0.0438, Figure 3C). These results suggest that quisqualate potentiates capsaicin-induced calcium elevation via changes in capsaicin efficacy and potency in DRG neurons. The quisqualate-induced potentiation was abolished by 30 μM MPEP ($F_{(3,40)}$ = 11.247, P = 0.771), but not 100 μM CPCCOEt (a selective negative allosteric modulator of $mGlu_1$ receptors; P < 0.0001, Figure 3D). In addition, application of DHPG, a selective $mGlu_{1/5}$ receptor agonist, enhanced capsaicin-induced calcium elevation ($F_{(1,26)}$ = 4.708, P = 0.039), while 10 μM AMPA, an AMPA/kainate receptor agonist, had no significant effect on responses to capsaicin ($F_{(1,22)}$ = 0.657, P = 0.426).

Cessation of activation of mGlu5 receptors attenuates capsaicin-induced $[Ca^{2+}]_i$ elevation in cultured DRG neurons

We examined the effects of capsaicin on intracellular calcium in DRG neurons after washout of glutamate and quisqualate (Figure 4). Interestingly, compared with neurons without glutamate or quisqualate application, the capsaicin-induced elevation of $[Ca^{2+}]_i$ was significantly decreased in neurons that had been previously exposed to glutamate ($F_{(1,144)}$ = 11.994, P = 0.007, Figure 4B and D) or quisqualate ($F_{(3,190)}$ = 7.004, P = 0.0007; Figure 4C and D). Changes in capsaicin E_{max} and EC_{50} were also evaluated after quisqualate washout (Figure 4F–H). Our analysis showed that the EC_{50} for capsaicin significantly increased during calcium elevation ($F_{(1,46)}$ = 8.491, P = 0.0055, Figure 4H), while E_{max} did not change ($F_{(1,46)}$ = 0.870, P = 0.3558, Figure 4G). These results suggest that cessation of quisqualate perfusion attenuates capsaicin-induced calcium elevation through changes in the potency of capsaicin. Quisqualate-induced calcium depletion was blocked by MPEP ($F_{(3,36)}$ = 8.300, P = 0.0012), but not CPCCOEt ($F_{(3,36)}$ = 8.300, P = 0.761, Figure 4E). In addition, application of DHPG decreased capsaicin-induced calcium elevation ($F_{(1,14)}$ = 12.842, P = 0.003), while AMPA had no significant effect on capsaicin response ($F_{(1,15)}$ = 0.664, P = 0.428). Therefore, cessation of the activation of $mGlu_5$ receptors inhibited capsaicin-induced calcium elevation in the mouse DRG neurons.

Quisqualate potentiates TRPV1-mediated calcium current in DRG neurons

Puff application of capsaicin (10 μM, 5 ms) from glass pipettes (8 MΩ) near DRG cell bodies (10–25 μm) resulted in large inward currents, at a holding potential of –60 mV (representative trace, Figure 5A). This response was completely blocked by addition of 1 μM 5'-IRTX (Figure 5B). Bath application of 10 μM quisqualate potentiated capsaicin-induced inward currents, which diminished after washout (quantitative data, Figure 5B). Quisqualate caused a significant increase in amplitude of capsaicin-induced currents ($F_{(2,13)}$ = 6.139, P = 0.028), but this effect disappeared after washout ($F_{(2,13)}$ = 1.519, P = 0.258). Increases in current amplitude were blocked by MPEP perfusion ($F_{(2,13)}$ = 6.139, P = 0.032). Thus, under voltage-clamp conditions, activation of $mGlu_5$ receptors enhanced TRPV1-mediated calcium currents, while inhibition of TRPV1-mediated calcium currents was not observed once $mGlu_5$ receptor activation was stopped. These changes in voltage-dependent components may contribute to the decrease in capsaicin-induced intracellular calcium response.

Quisqualate inhibits VGCCs in DRG neurons

To evaluate the contribution of VGCCs to the decreased response to capsaicin following activation of $mGlu_5$ receptors, we examined the effect of quisqualate on capsaicin-induced $[Ca^{2+}]_i$ in the presence of cadmium, a non-selective calcium channel blocker (Figure 6). In the presence of 0.1 mM cadmium chloride, we observed a decrease in the E_{max} of capsaicin ($F_{(3,58)}$ = 11.631, P = 0.041) and an increase in its EC_{50} ($F_{(3,58)}$ = 7.494, P = 0.021), suggesting that calcium channel components are involved in capsaicin-induced elevation of calcium. In the presence of cadmium, the
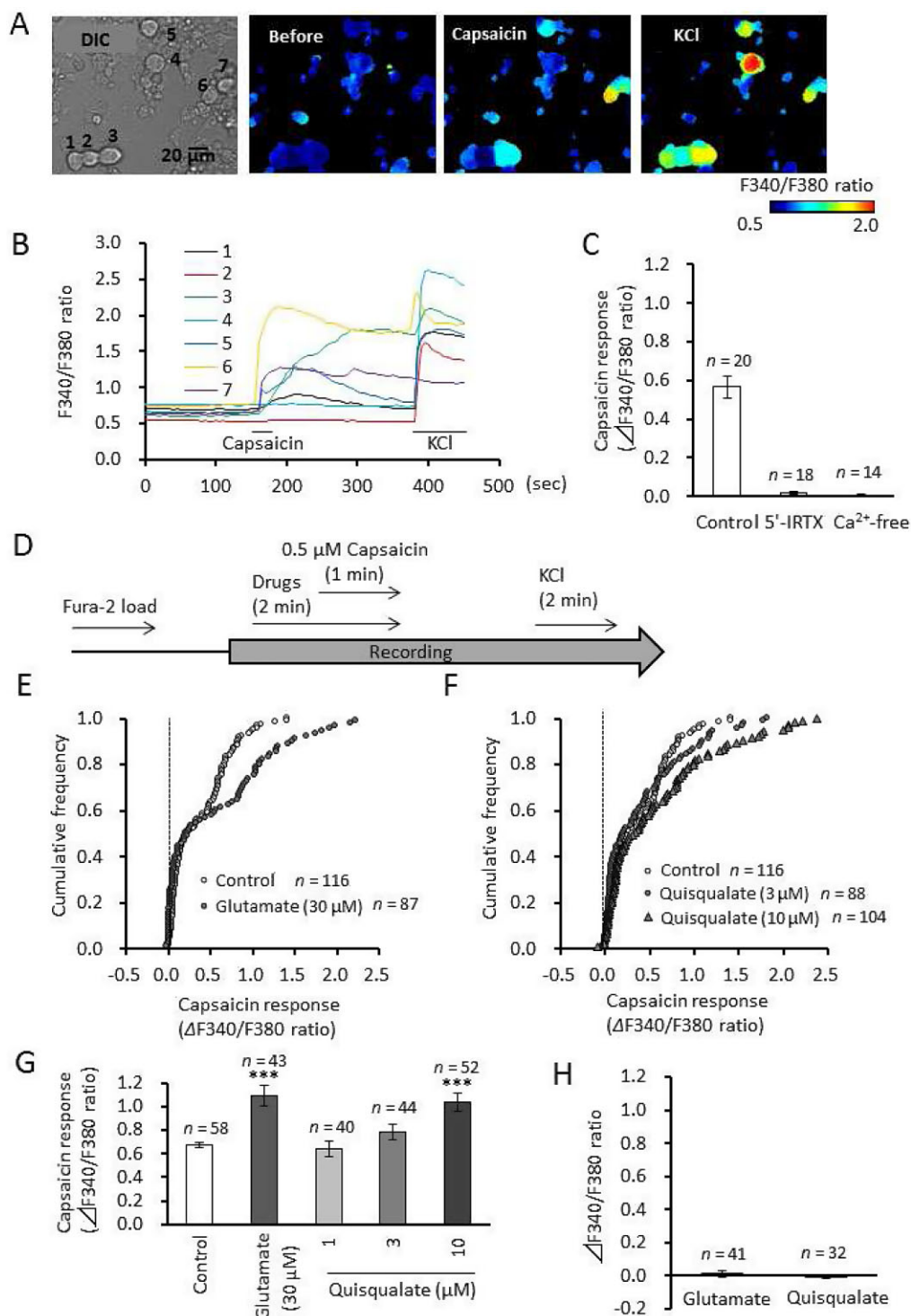
Figure 2

Effects of glutamatergic drug perfusion on capsaicin-induced elevation of intracellular calcium in primary cultured DRG neurons. (A) Representative images of F340/F380 ratio before and after the perfusion of capsaicin (0.5 μM) and KCl (50 mM) using Fra-2 AM dye. (B) Time course of F340/F380 ratio in seven independent cells from panel A. Horizontal bars represent periods of capsaicin and KCl perfusion. (C) Effects of 5′-IRTX and calcium-free solution on capsaicin-induced elevation of intracellular calcium in DRG neurons. (D) Experimental design for the recording of capsaicin-induced calcium elevation during glutamatergic drug perfusion. (E, F) Cumulative frequency graph showing changes in the F340/F380 ratio induced by capsaicin in the presence of glutamate and quisqualate. (G) Quantitative data showing changes in the F340/F380 ratio induced by capsaicin in the presence of glutamate and quisqualate. Data represents average of 50% of neurons, those with the largest capsaicin-induced calcium elevation. (H) Changes in intracellular calcium levels during glutamate or quisqualate perfusion. Data presented as mean ± SEM. ***$P < 0.0001$, significantly different from control.
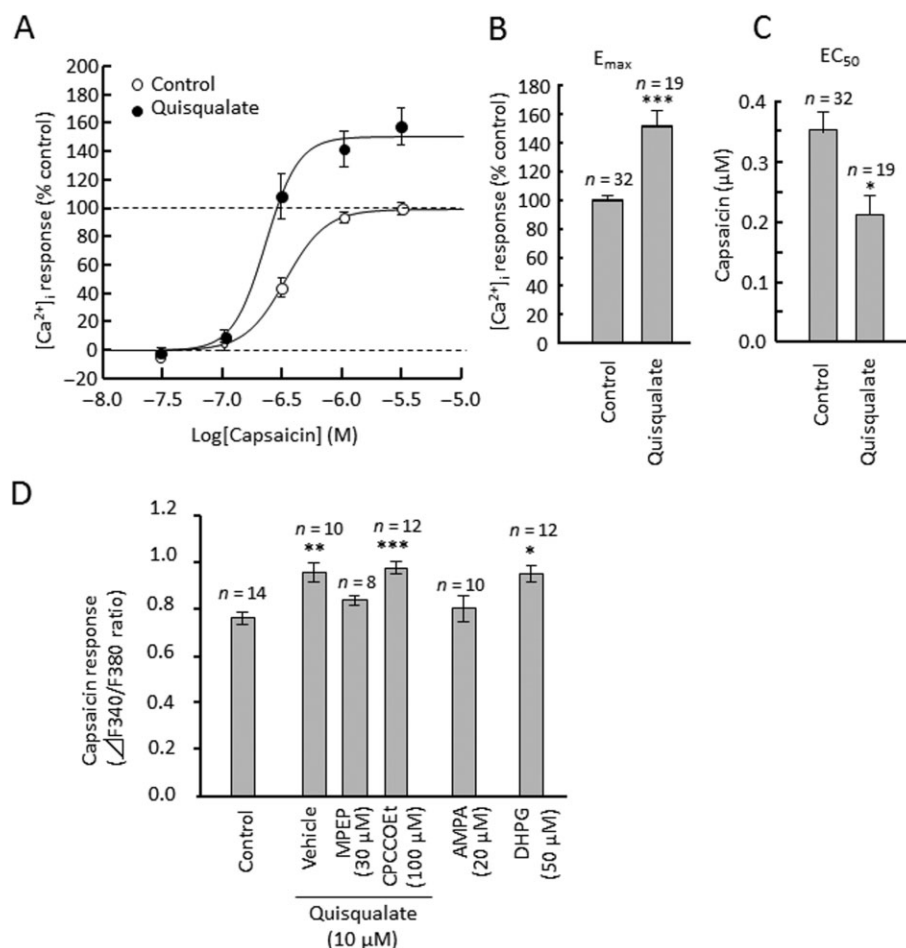
A

B

C

D

Figure 3

Pharmacological analysis of quisqualate-induced potentiation of capsaicin response in primary cultured DRG neurons (A) Concentration–response curves for capsaicin (0.03–3.0 μM) during quisqualate perfusion. Average E_{max} of capsaicin response (F340/F380 ratio) in the control group was defined as 100%. Summary of changes in E_{max} (B) and EC_{50} (C). (D) Quantitative data showing changes in the F340/F380 ratio induced by capsaicin, in the presence of glutamatergic drugs. Data represents average of 50% of neurons, those with the largest capsaicin-induced calcium elevation. Data presented as mean ± SEM. *$P < 0.05$, **$P < 0.01$, ***$P < 0.0001$, significantly different from control.

decrease in EC_{50} we had previously observed after quisqualate washout disappeared ($F_{(3,58)} = 7.494$, $P = 0.118$); instead, we detected an increase in E_{max} ($F_{(3,58)} = 11.631$, $P = 0.008$) and a decrease in EC_{50} ($F_{(3,58)} = 7.494$, $P < 0.0001$) during quisqualate perfusion. Next, we examined the effects of quisqualate on VGCC currents in DRG neurons. VGCC currents were evoked by depolarizing cells from −70 to +70 mV for 80 ms, from a holding potential of −80 mV. Representative traces of VGCC currents in DRG neurons, in response to capsaicin, are shown in Figure 7. Quisqualate (10 μM) caused a persistent decrease in VGCC currents between washouts. Figure 7E and F show the current densities of peak VGCC currents induced by depolarizing cells to +10 mV, from a holding potential of −80 mV, in capsaicin-sensitive and insensitive neurons respectively. VGCC currents in capsaicin-sensitive neurons were significantly inhibited during, and following, quisqualate perfusion ($F_{(2,18)} = 5.076$, $P = 0.047$ and $P = 0.037$, respectively, Figure 7E and Supporting Information Fig. S2). These effects disappeared with simultaneous perfusion of MPEP ($F_{(2,13)} = 0.120$, $P = 0.865$, Figure 7E). On the other hand,

quisqualate caused no significant changes in VGCC currents in capsaicin-insensitive neurons ($F_{(2,18)} = 0.282$, $P = 0.8115$) even after washout ($P = 0.8229$, Figure 7F). This difference may arise because of composition of the calcium channels, as the current–voltage (I–V) relationship in VGCC currents in capsaicin-sensitive neurons was different from that in capsaicin-insensitive neurons (Figure 7C and D).

Discussion and conclusions

In general, activation of TRPV1 channels caused inward currents, resulting in depolarization and subsequent VGCC activation, which in turn resulted in a large elevation in $[Ca^{2+}]_i$. The main finding of the present study was that activation of mGlu₅ receptors altered the TRPV1 channel-mediated $[Ca^{2+}]_i$ response in DRG neurons, which is caused by activity changes in both TRPV1 channels and VGCC currents. Activation of mGlu₅ receptors potentiated TRPV1 channel activity and inhibited VGCC currents. In total, TRPV1-mediated
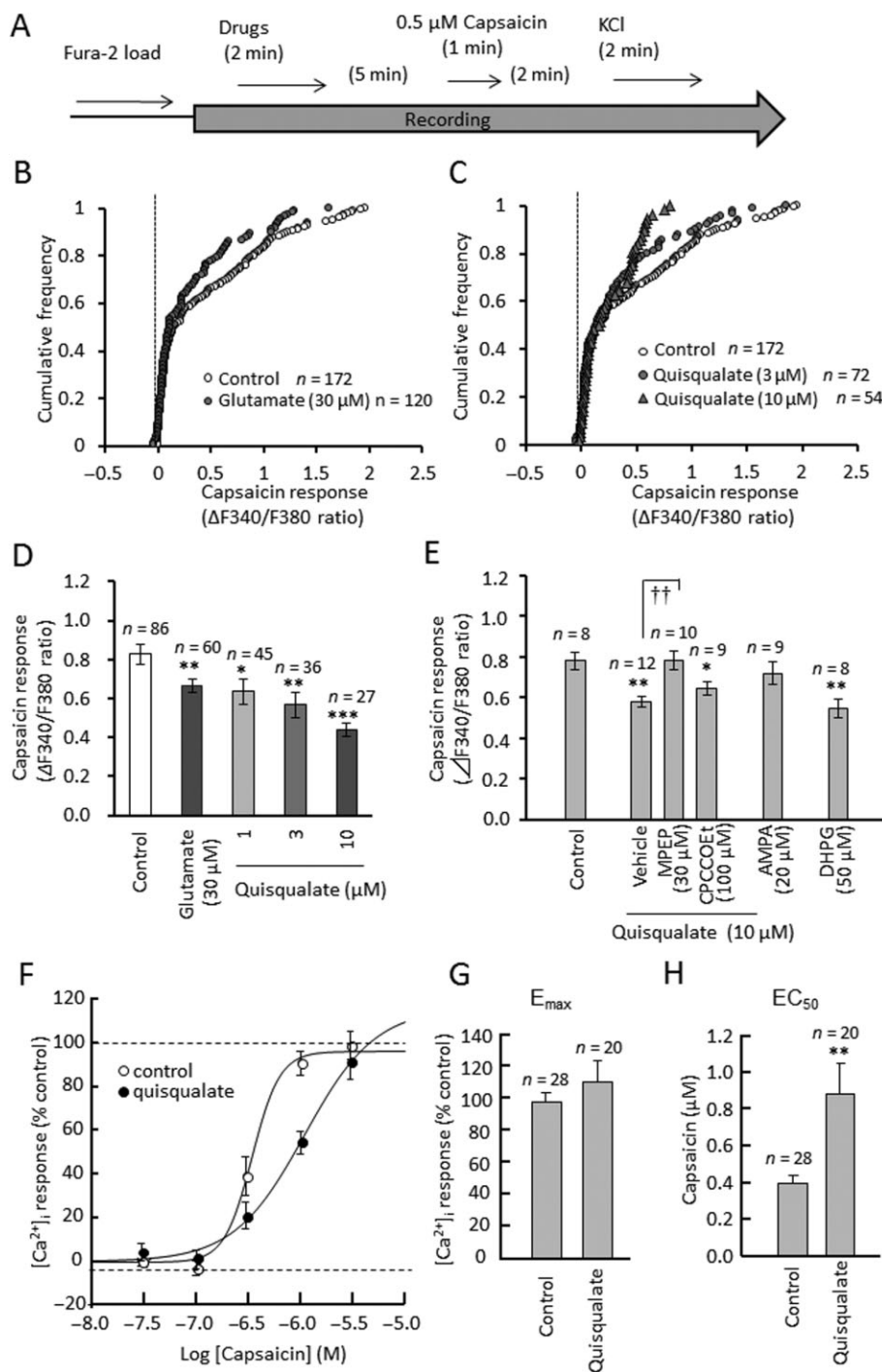
Figure 4

Effects of cessation of glutamatergic drug on capsaicin-induced intracellular calcium elevation in primary cultured DRG neurons. (A) Experimental design for recording capsaicin-induced calcium elevation after washout of glutamatergic drugs. (B, C) Cumulative frequency graph showing changes in the F340/F380 ratio induced by capsaicin after washout of glutamate and quisqualate. (D, E) Quantitative data showing changes in the F340/F380 ratio induced by capsaicin after washout of glutamatergic drugs. Data represent average of 50% of neurons, those with the largest capsaicin-induced calcium elevation. (F–H) Pharmacological analysis of quisqualate-induced depression of capsaicin response in primary cultured DRG neurons. (F) Concentration–response curves of capsaicin (0.03–3.0 μM) after washout of quisqualate. The average E_{max} for capsaicin ($\triangle$F340/F380 ratio) in control group was defined as 100%. Summary of changes in E_{max} (G) and EC_{50} (H). Data presented as mean ± SEM. *$P < 0.05$, **$P < 0.01$, ***$P < 0.0001$, significantly different from control, ††$P < 0.01$, significantly different as indicated.
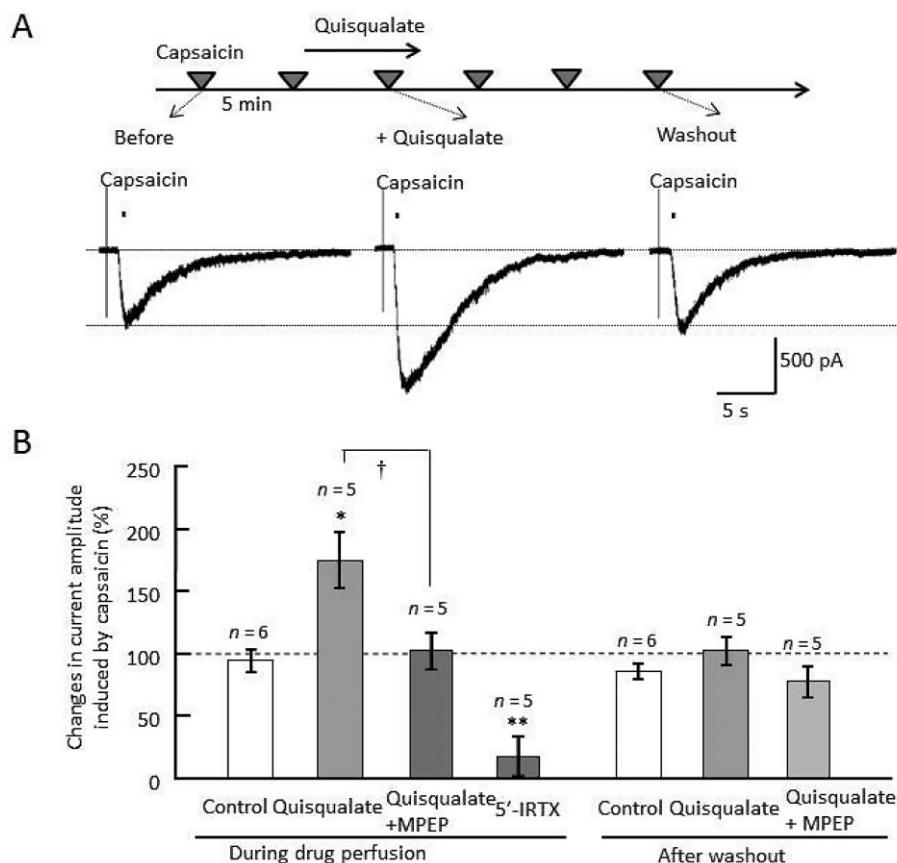
Figure 5

Effect of quisqualate on capsaicin-induced TRPV1 currents under voltage clamp conditions. (A) Experimental design for recording of capsaicin-induced currents. Original current traces were evoked by puff application of 10 µM capsaicin near the cell body, at a holding potential of −60 mV. All representative traces were recorded from single neurons, before, during and after (washout) quisqualate application. (B) Changes in amplitude of capsaicin-induced currents. The current amplitude in each cell was normalized to that of the capsaicin response prior to drug perfusion. Data presented as mean ± SEM. *$P < 0.05$, **$P < 0.01$ significantly different from control, †$P < 0.05$.

[Ca^{2+}]$_i$ elevation was potentiated, because TRPV1 channel potentiation was seemingly larger than VGCC current inhibition. Cessation of mGlu$_5$ receptor activation caused the TRPV1-induced increase in [Ca^{2+}]$_i$ to disappear, while VGCC current inhibition persisted. Thus, overall, TRPV1-mediated [Ca^{2+}]$_i$ elevation was reduced. The changes we have described in these responses mediated by TRPV1 channels may contribute to heat hyper- and hypoalgesia in mice.

Activation of mGlu$_5$ receptors potentiated TRPV1 channel-mediated [Ca^{2+}]$_i$ elevation. During activation of mGlu$_5$ receptors, the TRPV1 channel-mediated membrane current was enhanced. Several studies have found that mGluR5 activation facilitates TRPV1 channel trafficking and activity. Morenilla-Palao et al. (2004) reported that PKC activation, induced by mGlu$_5$ receptors, caused rapid delivery of functional TRPV1 channels to the plasma membrane and potentiated TRPV1 channel currents in oocytes co-expressing TRPV1 channels and mGlu$_5$ receptors. Bhave et al. (2003) reported that phosphorylation of TRPV1 channels, induced by PKC activation, sensitized these channels. On the other hand, increased levels of PI 4,5-bisphosphate (PIP$_2$) resulted in inhibition of TRPV1 channels (Lukacs et al., 2007), suggest-

ing that phospholipase C (PLC) activation by mGlu$_5$ receptors may be a consequence of PIP$_2$-mediated TRPV1 channel inhibition. It has been reported that activation of mGlu$_5$ receptors causes an increase in [Ca^{2+}]$_i$ in cultured DRG neurons (Crawford et al., 2000) and that these calcium responses are mediated by the activation of TRPV1 channels, which is induced by PKA or COX activation in mice (Hu et al., 2002) or diacylglycerol production in rats (Kim et al., 2009). However, mGlu$_5$ receptor-induced calcium responses were not detected in mouse cultured DRG neurons in the present study. Hu et al. (2002) used cultured DRG neurons that were dissected from 6 to 7-week-old mice and cultured for 6–7 days, and we used neurons that were dissected from 6 to 14-day-old mice and cultured for 2–3 days. We suggest that the expression and/or localization of the molecules contribute to the interactions between mGlu$_5$ receptors and the TRPV1 channel changes. The use of different species, ages and/or incubation stages of culture may have resulted in the disappearance of the intracellular calcium increases that was observed in the present study.

Removing the agonist after activation of mGlu$_5$ receptors caused a significant decrease in the degree of
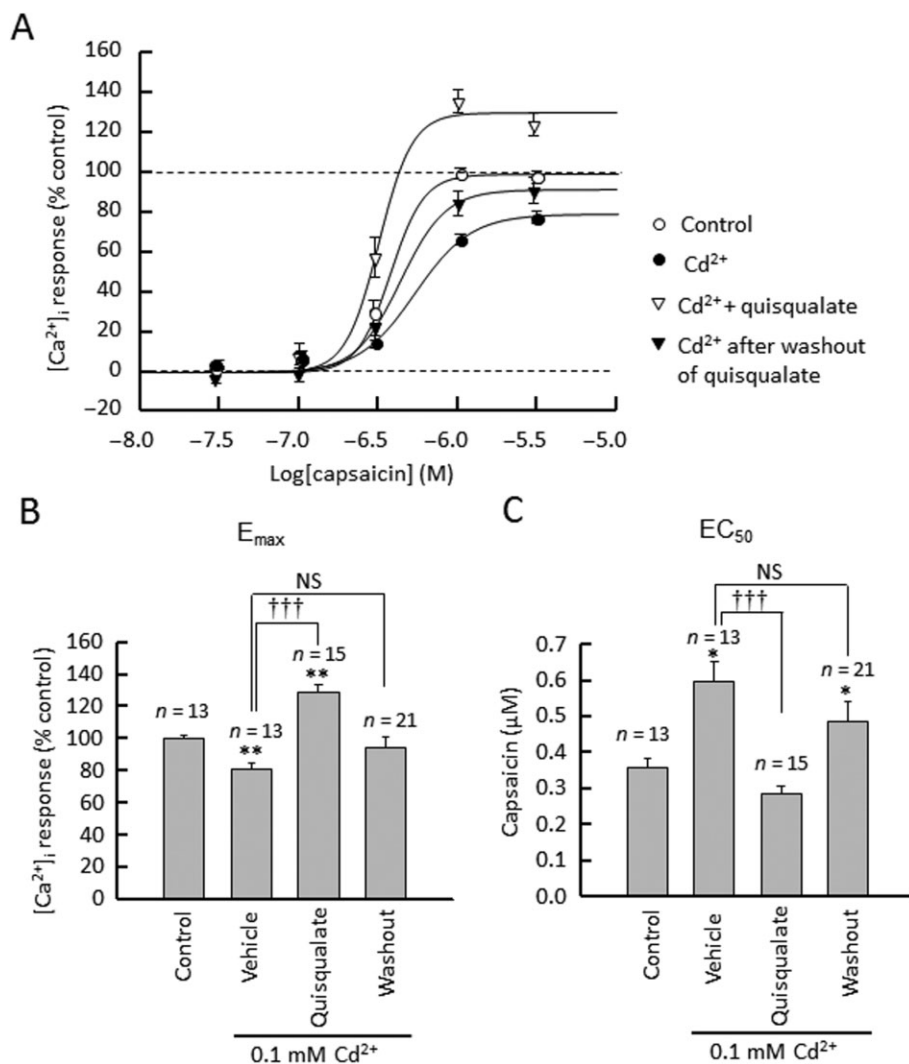
Figure 6
Effects of cadmium (Cd^{2+}) on quisqualate's biphasic modulation of capsaicin-induced calcium elevation (A) Concentration–response curves of capsaicin (0.03–3.0 µM) during or after quisqualate perfusion in presence of cadmium. The average E_{max} of capsaicin responses (F340/F380 ratio) in control group was defined as 100%. Summary of changes in E_{max} (B) and EC_{50} (C). Data presented as mean ± SEM. *$P < 0.05$, **$P < 0.01$ significantly different from control, †††$P < 0.001$, significantly different as indicated.

TRPV1-mediated calcium elevation, although the decrease in TRPV1 channel current was not observed under voltage-clamp conditions. On the other hand, VGCC currents in DRG neurons were inhibited by $mGlu_5$ receptor activation in capsaicin-sensitive neurons, even after cessation of activation of these receptors. Many studies have suggested that metabotropic receptors may contribute to VGCC current modulation. The application of mGlu receptor agonists reduced L-type VGCC currents in cultured hippocampal and neocortical neurons (Sayer *et al.*, 1992; Sahara and Westbrook, 1993). Gamper *et al.* (2004) reported that the depletion of PIP_2, activated by $G_{q/11}$ protein-coupled muscarinic M_1 receptors, caused suppression of N-type calcium currents in superior cervical ganglion (SCG) neurons. Liu *et al.* (2004) reported that inhibition of L- and N-type calcium channels by M_1 receptor activation in SCG neurons was mediated by diacylglycerol lipase activation. Interestingly, mGluR5a acti-

vation can also cause biosynthesis of 2-arachidonoylglycerol, an endocannabinoid, resulting in N-type calcium channel inhibition via the activation of cannabinoid CB_1 receptors in cultured SCG neurons (Won *et al.*, 2009).

Scroggs and Fox (1992) reported that, in rat DRG neurons, the distribution of calcium channel subtypes was dependent on cell diameter. For instance, the percentage of L-type calcium channels was significantly larger in small diameter neurons (52.9% of total whole-cell calcium channels) than in medium- and large-diameter neurons (6.6 and 19.4% of total whole-cell calcium channels, respectively). In contrast, the percentage of N-type calcium channels was similar in small-, medium- and large-diameter neurons. Almost all capsaicin-sensitive neurons in the DRG are classified as small- and medium-sized neurons (Kobayashi *et al.*, 2005); therefore, activation of $mGlu_5$ receptors may inhibit a type of VGCC current that is predominantly expressed in capsaicin-
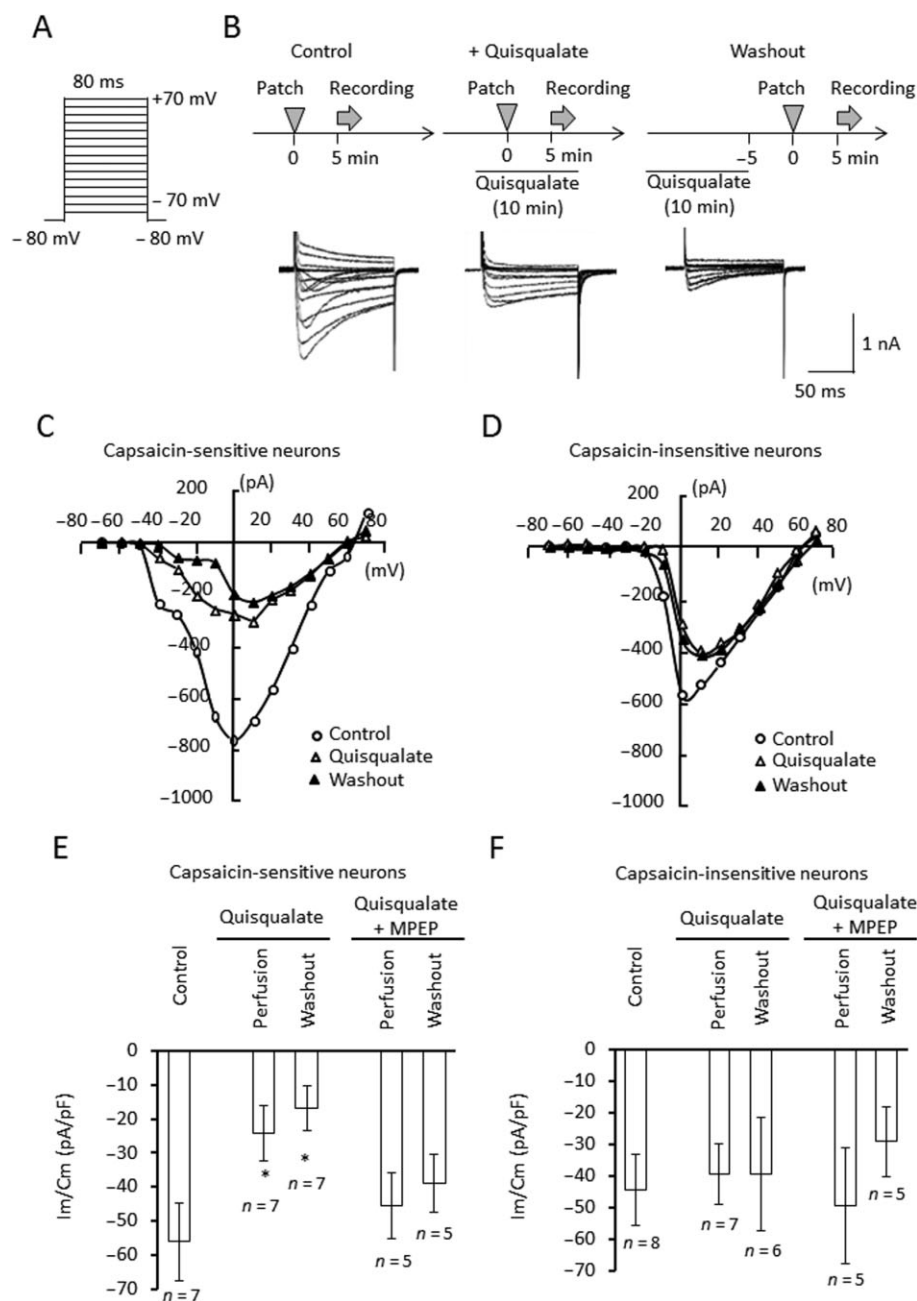
Figure 7

Effects of quisqualate on voltage-gated calcium channels in DRG neurons. (A) Calcium currents (I_{Ca}) were evoked *via* depolarization from −70 to +70 mV, for 80 ms, from a holding potential of−80 mV. (B) Original I_{Ca} traces before, during and after (washout) quisqualate application. Current responses were measured once from each neuron. Current–voltage relationships in capsaicin-sensitive (C) and insensitive (D) DRG neurons, under control, quisqualate or quisqualate washout conditions. Quantitative data on current densities induced by a 10 mV depolarization step in capsaicin-sensitive (E) and insensitive (F) DRG neurons. I_m, whole-cell current, C_m, membrane capacitance, Data presented as mean ± SEM. *$P < 0.05$, significantly different from control.

sensitive neurons. In the present study, mGlu$_5$ receptor-induced inhibition of VGCC currents was persistent. It is well understood that activation of mGlu$_{1/5}$ receptors can regulate internalization and translation of several molecules via at least two signal transduction pathways (ERK and mammalian target of rapamycin), resulting in long-term synaptic depression in the hippocampus (Snyder *et al.*, 2001; Banko *et al.*,

2006). Therefore, mGlu$_{1/5}$ receptors may also regulate internalization or translation of VGCC regulating molecules in DRG neurons.

We have shown that activation of mGlu$_5$ receptors contributes to heat hyper- and hypoalgesia in mouse hind paws. Acute mGluR5 activation produced heat hyperalgesia *in vivo*, which correlated with sensitization of TRPV1 channel

responses in the presence of quisqualate in DRG neurons *in vitro*. Similar effects have been observed in rats, as an intraplantar injection of DHPG increased sensitivity to thermal and mechanical stimuli (Jung *et al.*, 2011). Furthermore, novel and unique observations were found during the chronic phase, as heat hypoalgesia, mediated by mGlu$_5$ receptor stimulation, was observed 4 h after quisqualate injection. Hypoalgesia caused by quisqualate *in vivo* may correlate with the reduction in TRPV1-mediated $[Ca^{2+}]_i$ elevation after quisqualate washout seen *in vitro*, perhaps because of the metabolism or dilution of quisqualate in paw tissue. On the other hand, intraplantar quisqualate caused mechanical hypersensitivity, but did not reduce mechanosensitivity. Mechanoreceptor neurons co-express degerin/epithelial Na^+ channels and TRP (TRPV3, TRPV4 or TRPA1) channel proteins that, together, form mechano-electrical transduction (MeT) channels (Geffeney and Goodman, 2012). Mechanical hyperalgesia induced by intraplantar quisqualate may be caused by a TRPV1-independent mechanism, such as MeT channel regulation.

Recently, Kumar *et al.* (2012) reported that functional mGlu$_5$ receptors were expressed not only on neuronal cell surfaces, but also in intracellular membranes, such as the endoplasmic reticulum, Golgi and nuclear membranes. Quisqualate has been reported to be able to pass through cell membranes and activate both cell surface and intracellular receptors, whereas DHPG only activates cell surface receptors (Kumar *et al.*, 2012). As quisqualate and DHPG had the same effect on $[Ca^{2+}]_i$ in the present study, it may be that activation of cell surface mGlu$_5$ receptors are responsible for the potentiation and attenuation of TRPV1-mediated $[Ca^{2+}]_i$ in mouse DRG neurons.

In conclusion, activation of mGlu$_5$ receptors had biphasic effects on TRPV1-mediated $[Ca^{2+}]_i$ elevation in mouse DRG neurons. These effects were due to the transient potentiation of TRPV1 channel currents and the persistent inhibition of VGCC currents by TRPV1-mediated depolarization. These phenomena may contribute to the modulation of sensitivity to noxious heat.

Acknowledgements

Author contribution

T. M. designed the study. T. M., T. N., M. K., Y. T. and N. I. performed the research and analysed data. T. M., J. Y., N. K., T. I. and M. N. wrote the paper.

Conflict of interest

None.

References

Abe T, Sugihara H, Nawa H, Shigemoto R, Mizuno N, Nakanishi S (1992). Molecular characterization of a novel metabotropic glutamate receptor mGluR5 coupled to inositol phosphate/Ca2+ signal transduction. J Biol Chem 267: 13361–13368.

Alexander SPH, Benson HE, Faccenda E, Pawson AJ, Sharman JL, Spedding M *et al.* (2013a). The Concise Guide to PHARMACOLOGY 2013/14: G Protein-Coupled Receptors. Br J Pharmacol 170: 1459–1581.

Alexander SPH, Benson HE, Faccenda E, Pawson AJ, Sharman JL, Spedding M *et al.* (2013b). The Concise Guide to PHARMACOLOGY 2013/14: Ion Channels. Br J Pharmacol 170: 1607–1651.

Alexander SPH, Benson HE, Faccenda E, Pawson AJ, Sharman JL, Spedding M *et al.* (2013c). The Concise Guide to PHARMACOLOGY 2013/14: Ligand-Gated Ion Channels. Br J Pharmacol 170: 1582–1606.

Banko JL, Hou L, Poulin F, Sonenberg N, Klann E (2006). Regulation of eukaryotic initiation factor 4E by converging signaling pathways during metabotropic glutamate receptor-dependent long-term depression. J Neurosci 26: 2167–2173.

Bhave G, Karim F, Carlton SM, Gereau RW 4th (2001). Peripheral group I metabotropic glutamate receptors modulate nociception in mice. Nat Neurosci 4: 417–423.

Bhave G, Hu HJ, Glauner KS, Zhu W, Wang H, Brasier DJ *et al.* (2003). Protein kinase C phosphorylation sensitizes but does not activate the capsaicin receptor transient receptor potential vanilloid 1 (TRPV1). Proc Natl Acad Sci U S A 100: 12480–12485.

Callaghan B, Haythornthwaite A, Berecki G, Clark RJ, Craik DJ, Adams DJ (2008). Analgesic alpha-conotoxins Vc1.1 and Rg1A inhibit N-type calcium channels in rat sensory neurons *via* GABAB receptor activation. J Neurosci 28: 10943–10951.

Caterina MJ, Schumacher MA, Tominaga M, Rosen TA, Levine JD, Julius D (1997). The capsaicin receptor: a heat-activated ion channel in the pain pathway. Nature 389: 816–824.

Chaplan SR, Bach FW, Pogrel JW, Chung JM, Yaksh TL (1994). Quantitative assessment of tactile allodynia in the rat paw. J Neurosci Methods 53: 55–63.

Chiechio S, Nicoletti F (2012). Metabotropic glutamate receptors and the control of chronic pain. Curr Opin Pharmacol 12: 28–34.

Crawford JH, Wainwright A, Heavens R, Pollock J, Martin DJ, Scott RH *et al.* (2000). Mobilisation of intracellular Ca^{2+} by mGluR5 metabotropic glutamate receptor activation in neonatal rat cultured dorsal root ganglia neurons. Neuropharmacology 39: 621–630.

Dölen G, Osterweil E, Rao BS, Smith GB, Auerbach BD, Chattarji S *et al.* (2007). Correction of fragile X syndrome in mice. Neuron 56: 955–962.

Gamper N, Reznikov V, Yamada Y, Yang J, Shapiro MS (2004). Phosphatidylinositol [correction] 4,5-bisphosphate signals underlie receptor-specific Gq/11-mediated modulation of N-type Ca^{2+} channels. J Neurosci 24: 10980–10992.

Geffeney SL, Goodman MB (2012). How we feel: ion channel partnerships that detect mechanical inputs and give rise to touch and pain perception. Neuron 74: 609–619.

Guo W, Wei F, Zou S, Robbins MT, Sugiyo S, Ikeda T et al. (2004). Group I metabotropic glutamate receptor NMDA receptor coupling and signaling cascade mediate spinal dorsal horn NMDA receptor 2B tyrosine phosphorylation associated with inflammatory hyperalgesia. J Neurosci 24: 9161–9173.

Han P, Korepanova AV, Vos MH, Moreland RB, Chiu ML, Faltynek CR (2013). Quantification of TRPV1 protein levels in rat tissues to understand its physiological roles. J Mol Neurosci 50: 23–32.

Hu HJ, Bhave G, Gereau RW 4th. (2002). Prostaglandin and protein kinase A-dependent modulation of vanilloid receptor function by metabotropic glutamate receptor 5: potential mechanism for thermal hyperalgesia. J Neurosci 22: 7444–7452.

Hudson LJ, Bevan S, McNair K, Gentry C, Fox A, Kuhn R et al. (2002). Metabotropic glutamate receptor 5 upregulation in A-fibers after spinal nerve injury: 2-methyl-6-(phenylethynyl)-pyridine (MPEP) reverses the induced thermal hyperalgesia. J Neurosci 22: 2660–2668.

Jung SS, Sung KW, Lee SE, Shin HK (2011). Capsaicin prevents the hyperalgesia induced by peripheral group I mGluRs activation. Neurosci Lett 500: 197–201.

Kew JN, Kemp JA (2005). Ionotropic and metabotropic glutamate receptor structure and pharmacology. Psychopharmacology (Berl) 179: 4–29.

Kilkenny C, Browne W, Cuthill IC, Emerson M, Altman DG (2010). Animal research: reporting in vivo experiments: the ARRIVE guidelines. Br J Pharmacol 160: 1577–1579.

Kim YH, Park CK, Back SK, Lee CJ, Hwang SJ, Bae YC et al. (2009). Membrane-delimited coupling of TRPV1 and mGluR5 on presynaptic terminals of nociceptive neurons. J Neurosci 29: 10000–10009.

Kobayashi K, Fukuoka T, Obata K, Yamanaka H, Dai Y, Tokunaga A et al. (2005). Distinct expression of TRPM8, TRPA1, and TRPV1 mRNAs in rat primary afferent neurons with adelta/c-fibers and colocalization with trk receptors. J Comp Neurol 493: 596–606.

Kumar V, Fahey PG, Jong YJ, Ramanan N, O'Malley KL (2012). Activation of intracellular metabotropic glutamate receptor 5 in striatal neurons leads to up-regulation of genes associated with sustained synaptic transmission including Arc/Arg3.1 protein. J Biol Chem 287: 5412–5425.

Lawand NB, McNearney T, Westlund KN (2000). Amino acid release into the knee joint: key role in nociception and inflammation. Pain 86: 69–74.

Li JQ, Chen SR, Chen H, Cai YQ, Pan HL (2010). Regulation of increased glutamatergic input to spinal dorsal horn neurons by mGluR5 in diabetic neuropathic pain. J Neurochem 112: 162–172.

Liu L, Roberts ML, Rittenhouse AR (2004). Phospholipid metabolism is required for M1 muscarinic inhibition of N-type calcium current in sympathetic neurons. Eur Biophys J 33: 255–264.

Liu MG, Matsuura S, Shinoda M, Honda K, Suzuki I, Shibuta K et al. (2012). Metabotropic glutamate receptor 5 contributes to inflammatory tongue pain via extracellular signal-regulated kinase signaling in the trigeminal spinal subnucleus caudalis and upper cervical spinal cord. J Neuroinflammation 9: 258.

Liu XJ, Salter MW (2010). Glutamate receptor phosphorylation and trafficking in pain plasticity in spinal cord dorsal horn. Eur J Neurosci 32: 278–289.

Lukacs V, Thyagarajan B, Varnai P, Balla A, Balla T, Rohacs T (2007). Dual regulation of TRPV1 by phosphoinositides. J Neurosci 27: 7070–7080.

McGrath JC, Drummond GB, McLachlan EM, Kilkenny C, Wainwright CL (2010). Guidelines for reporting experiments involving animals: the ARRIVE guidelines. Br J Pharmacol 160: 1573–1576.

Ménard C, Quirion R (2012). Group 1 metabotropic glutamate receptor function and its regulation of learning and memory in the aging brain. Front Pharmacol 3: 182.

Mitchell K, Lebovitz EE, Keller JM, Mannes AJ, Nemenov MI, Iadarola MJ (2014). Nociception and inflammatory hyperalgesia evaluated in rodents using infrared laser stimulation after Trpv1 gene knockout or resiniferatoxin lesion. Pain 155: 733–745.

Morenilla-Palao C, Planells-Cases R, García-Sanz N, Ferrer-Montiel A (2004). Regulated exocytosis contributes to protein kinase C potentiation of vanilloid receptor activity. J Biol Chem 279: 25665–25672.

Omote K, Kawamata T, Kawamata M, Namiki A (1998). Formalin-induced release of excitatory amino acids in the skin of the rat hindpaw. Brain Res 787: 161–164.

Pawson AJ, Sharman JL, Benson HE, Faccenda E, Alexander SP, Buneman OP et al.; NC-IUPHAR (2014). The IUPHAR/BPS Guide to PHARMACOLOGY: an expert-driven knowledge base of drug targets and their ligands. Nucl. Acids Res 42 (Database Issue): D1098–1106.

Sahara Y, Westbrook GL (1993). Modulation of calcium currents by a metabotropic glutamate receptor involves fast and slow kinetic components in cultured hippocampal neurons. J Neurosci 13: 3041–3050.

Sayer RJ, Schwindt PC, Crill WE (1992). Metabotropic glutamate receptor-mediated suppression of L-type calcium current in acutely isolated neocortical neurons. J Neurophysiol 68: 833–842.

Scroggs RS, Fox AP (1992). Calcium current variation between acutely isolated adult rat dorsal root ganglion neurons of different size. J Physiol 445: 639–658.

Snyder EM, Philpot BD, Huber KM, Dong X, Fallon JR, Bear MF (2001). Internalization of ionotropic glutamate receptors in response to mGluR activation. Nat Neurosci 4: 1079–1085.

Stawski P, Janovjak H, Trauner D (2010). Pharmacology of ionotropic glutamate receptors: a structural perspective. Bioorg Med Chem 18: 7759–7772.

Walker K, Reeve A, Bowes M, Winter J, Wotherspoon G, Davis A et al. (2001). mGlu5 receptors and nociceptive function II. mGlu5 receptors functionally expressed on peripheral sensory neurones mediate inflammatory hyperalgesia. Neuropharmacology 40: 10–19.

Won YJ, Puhl HL 3rd, Ikeda SR (2009). Molecular reconstruction of mGluR5a-mediated endocannabinoid signaling cascade in single rat sympathetic neurons. J Neurosci 29: 13603–13612.

Yan LH, Hou JF, Liu MG, Li MM, Cui XY, Lu ZM et al. (2009). Imbalance between excitatory and inhibitory amino acids at spinal level is associated with maintenance of persistent pain-related behaviors. Pharmacol Res 59: 290–299.

Yoshida J, Ishibashi T, Imaizumi N, Takegami T, Nishio M (2005). Capacitative Ca^{2+} entries and mRNA expression for TRPC1 and TRPC5 channels in human epidermoid carcinoma A431 cells. Eur J Pharmacol 510: 217–222.

Supporting information

Additional Supporting Information may be found in the online version of this article at the publisher's web-site:

http://dx.doi.org/10.1111/bph.12962

Figure S1 Effects of intraplantar 5′-IRTX injection on hot plate response. Changes in latency to shake, lick, or jump after placement on hot plate (55.0 ± 0.2°C) (A) 15 min or (B) 4 h after 5′-IRTX injection (0.01 nmol per paw). Eight mice were used in each group. *$P < 0.05$ against control. Data is presented as mean ± SEM.

Figure S2 Time plot showing calcium current density in a representative capsaicin-sensitive DRG neuron. Calcium currents were evoked by depolarizing the cell in 10 mV, 20 ms steps, every 20 s, from a holding potential of −80 mV. The horizontal bar represents quisqualate (10 μM) perfusion. Black and red traces were recorded at time points indicated by the respective coloured arrows.